Available online at www.sciencedirect.com

SciVerse ScienceDirect

Journal of the European Ceramic Society 32 (2012) 2095–2102

www.elsevier.com/locate/jeurceramsoc

Effect of feldspar particle size on the porous microstructure and stain resistance of polished porcelain tiles

H.J. Alves *, F.G. Melchiades, A.O. Boschi

Laboratório de Revestimentos Cerâmicos (LaRC), Departamento de Engenharia de Materiais (DEMa), Universidade Federal de São Carlos (UFSCar), Rod. Washington Luiz, Km. 235, 13574-970 São Carlos, SP, Brazil

Received 19 September 2011; received in revised form 5 March 2012; accepted 12 March 2012
Available online 10 April 2012

Abstract

The final porosity of porcelain tiles results from the incomplete densification of the material during the stages of processing. The use of raw materials such as feldspar, with a high potential for forming liquid phase during sintering, contributes to eliminate porosity when a suitable heating cycle is employed. This paper presents the results of a study that investigated the effect of the particle size distribution (PSD) of feldspar on the formation of pores in the green compact and the final product, using stain resistance as an evaluation parameter of surface porosity. To this end, the feldspar used in a standard paste of technical porcelain was milled under different conditions to produce the desired changes in its PSD. The groundbreaking results indicate that slight changes in the milling conditions of feldspar can significantly alter the porous microstructure of the material and the stain resistance of the polished tile surface.

Keywords: Porcelain; Porosity; Milling; Feldspar; Microstructure-final

1. Introduction

Porcelain tile staining is caused by the presence of pores. The porosity of porcelain tiles is due mainly to the incomplete elimination of pores from the green compact during sintering.[1–4] Therefore, controlling the staining of porcelain tiles of a given composition requires focusing special attention on the porosity of the green compact and on its sintering conditions. With regard to the green compact, the volume and morphological characteristics of intragranular and intergranular pores depend, among other variables, on the particle size distribution (PSD) of the raw materials, the granulometric distribution of the spray-dried material and the compaction pressure.[5,6]

A recent study found that the granulometric distribution of spray-dried material does not interfere significantly in its pore size distribution after sintering, since distinct granulometric compositions led to the same porosity in the sintered product.[7] The milling yield of the porcelain bodies evaluated by Amorós et al. was related to the porosity of the green compact, the porosity of the final product and the stain resistance.[8] The aforementioned study found that insufficient milling (larger residue in a sieve with 45 μm openings) is responsible for producing green ceramic bodies with a wide pore size distribution and higher apparent density (higher packing). However, a wider pore size distribution implies the presence of pores with large diameters in the green compact, which impairs the sintering process because high temperatures are required to reach maximum densification, resulting in a product with low apparent density and low stain resistance.[5,6,8]

These pores are eliminated during sintering through liquid phase sintering. The most important raw material responsible for the amount, nature and characteristics of the liquid phase during sintering, and consequently the ability of a composition to eliminate pores in the green compact, is feldspar.[9,10] The PSD of feldspar affects the development of the green microstructure during compaction (pore volume and characteristics) and its reactivity during sintering. It is therefore a crucial variable in determining the staining of porcelain tiles.[11]

The objective of this work was to study the correlations between the PSD of feldspar, the characteristics of the pores in

* Corresponding author. Tel.: +55 16 33617980; fax: +55 16 33615404.
E-mail address: helquimica@yahoo.com.br (H.J. Alves).

0955-2219/$ – see front matter © 2012 Elsevier Ltd. All rights reserved.
doi:10.1016/j.jeurceramsoc.2012.03.019

Table 1
Formulation of the STD paste and the F1 composition.

Raw materials	STD (in wt.%)	F1[a] (in wt.%)
Feldspar	51.5	–
Clay I	18.4	38.0
Kaolin	14.5	30.0
Clay II	4.9	10.0
Alumina	3.9	8.0
Zirconite	3.9	8.0
Frit	2.9	6.0

[a] Formulation F1 (without feldspar) was readjusted while maintaining the proportions of the other components of the STD paste.

the green compact, the elimination of these pores during sintering, and the susceptibility to staining of sintered polished surfaces.

2. Materials and methods

This research used raw materials that make up the standard paste (STD) of a commercial polished porcelain tile whose formulation and chemical analysis are presented in Tables 1 and 2, respectively. The STD paste was evaluated previously by X-ray fluorescence (Philips MagiX Spectrometer). Several of the parameters used here were determined based on the information provided by the manufacturer of the product and the literature on the subject. The methodology adopted was designed to reveal the effect of the addition of feldspar with different PSD profiles on the properties of the STD paste. Thus, because the main objective was to analyze the variable of PSD separately, the chemical and mineralogical compositions of the raw materials were not examined.

2.1. Milling of the standard paste

The STD paste was initially obtained by dosing and mixing the raw materials previously dried at 110 °C for 24 h, in the proportions listed in Table 1. This composition was milled in a laboratory ball mill (Certech ST-242) to obtain a suspension with 60% (m/m) of water and a milling residue of about 0.5% after sifting through a sieve with 45 μm openings (parameter used by the manufacturer of the product). The milling time was 14 min and the other conditions of the experiment were standardized as follows: mill (1000 mL), load of alumina balls (600 g of large balls and 585 g of small balls), solids mass (300 g), water mass (180 g) and sodium silicate as a deflocculant (1.8 g). After milling was concluded, the mill was emptied and the density of the suspension (ρ_S) was determined using a stainless steel pycnometer (model 108 – tare 200). The suspension contained in the pycnometer was then sifted through the sieve with 45 μm openings to determine the milling residue by drying and weighing the particles retained in the mesh. Part of the original suspension (sifted through the sieve with 63 μm openings) was subjected to X-ray sedimentometry (Micromeritics Sedigraph 5000 D) to determine its PSD. The remainder of the suspension was dried in an electric oven at 110 °C for 24 h. After drying, the absolute density of the solids (ρ_R) was determined by helium pycnometry (Quantachrome Ultrapycnometer 1000).

Table 2
Chemical analysis of the STD paste.

Oxides (%)	STD
P.F.	3.37
SiO_2	56.91
Al_2O_3	23.61
Fe_2O_3	0.28
TiO_2	0.10
CaO	1.07
MgO	0.43
K_2O	0.96
Na_2O	2.42
Li_2O	0.54
ZrO_2	10.16
P_2O_5	0.15

2.2. Milling of the feldspar

The methodology applied in this phase of the work was divided into three stages:

Stage 1: The feldspar was milled individually under the same conditions as those described in Section 2.1, using three different milling times (21.0 min, 18.5 min and 12.5 min) to obtain different residues in a sieve with 45 μm openings. The resulting suspensions were analyzed to determine the ρ_S, ρ_R, milling residue and PSD.

Stage 2: Concomitantly, a STD suspension was prepared containing no feldspar, which was denoted as F1. To this end, the STD composition was altered by excluding this raw material, and therefore required an adjustment, maintaining the proportions found originally among the other initial components, as indicated in Table 1. Composition F1 was milled for 12.0 min to obtain a residue of less than 0.5% retained in the sieve with 45 μm openings, i.e., close to the amount of residue of the STD paste. The values of ρ_S and ρ_R in F1 were determined.

Stage 3: After preparing the feldspar suspension under the milling conditions described in Stage 1, the procedure consisted of mixing the three different residues individually into the F1 suspension by means of quantitative volumetric addition to reproduce the initial STD formulation (Table 1). For this purpose the calculations were based on Eq. (1), where M_S is the dry mass of solids present in a given volume V_S of suspension.

$$M_S = V_S \cdot \rho_R \left(\frac{\rho_S - 1}{\rho_R - 1} \right) \quad (1)$$

Thus, knowing the mass of solids in a given volume of suspension, it was possible to determine the required volume of each suspension that should be mixed in order to reproduce the initial STD formulation.

Before and after each volumetric mixture, the suspensions were kept under mechanical shaking for 15 min, at a rotation of 800 rpm. Part of the volume of the suspensions was then analyzed to determine the PSD. The remaining volumes of these suspensions were dried at 110 °C for 24 h, and the resulting pastes were used for the preparation of green bodies.

2.3. Preparation and characterization of the green bodies

After drying the suspensions, the green bodies were prepared according to the procedures described below.

The solid materials were carefully ground in a porcelain mortar until they passed completely through a sieve of opening of sieve with 355 μm openings. The powders were moisturized with 5 wt.% water (dry weight basis) and granulated by sifting through a sieve with 600 μm openings. The sieving procedure was repeated three times to ensure the homogeneity and quality of the granulation. The granulated powders were stored in separate plastic bags and allowed to "rest" for 24 h. For each evaluated condition, green bodies were prepared with dimensions of 6.0 cm × 2.0 cm by pressing the granulated powders under a uniaxial pressure of 44 MPa, using an automatic press (Nannetti, Mignon SS/EA). The green bodies were dried at 110 °C until they reached a constant weight, after which they were analyzed by the geometric method to determine their apparent density (ρ_C), and by mercury porosimetry (Micromeritics AutoPore III) to characterize their porosity.

2.4. Sintering, characterization of the final porosity and evaluation of staining

The green bodies were sintered in an electric lab furnace, using a heating cycle of approximately 55 min, a heating rate of 45 °C/min, a dwell time of 8 min at the maximum temperature, and a cooling rate of 60 °C/min to room temperature.

The sintering temperature (T_{max}) of the green bodies of each evaluated condition was chosen according to its maximum densification, based on the highest linear firing shrinkage (LS) and lowest water absorption (WA) presented at four different previously selected temperatures.

The following values were determined after sintering:

- WA, by the boiling water method for during 2 h, according to the ISO 10545-3 standard[12];
- apparent porosity (ε_A) by the Archimedes principle;
- total porosity (ε) and closed porosity (ε_F), by means of equations:

$$\varepsilon = 1 - \left(\frac{\rho_{CS}}{\rho_{RS}}\right) \quad (2)$$

$$\varepsilon_F = \varepsilon - \varepsilon_A \quad (3)$$

where ρ_{CS} is the apparent density and ρ_{RS} the absolute density of the solid obtained after sintering; and

- degree of densification (ϕ), defined as:

$$\phi = \left(\frac{\rho_{CS}}{\rho_{RS}}\right) \quad (4)$$

Ten test specimens of each green body evaluated were used for the porosity tests.

Small samples with dimensions of 1.5 cm × 1.5 cm × 0.5 cm were then precision cut from the sintered compacts, using a diamond cutting disc. These samples were cleaned ultrasonically for 20 min and dried at 110 °C for 24 h, after which they were sandpapers and polished using an automatic system with water, composed of a rotary disc and a series of five polishing pads of silicon carbide with abrasives #60, #200, #600, #1000 and #1200 (nominal grit numbers) to simulate the industrial polishing process. The samples were polished for 15 min with each pad, resulting in surfaces prepared under the same conditions.[13–15]

The characteristics of the samples' surface microstructure after polishing were determined from digital images (micrographs) obtained with a scanning electron microscope (SEM, Leo Stereoscan 440). The micrographs were analyzed using the Image-Pro 4.5 software program, which allowed for the determination of the percentage corresponding to the area covered by pores in relation to the total area of the analyzed images, their diameter distribution, and aspects related to their morphology (aspect ratio). The area of each analyzed image was 0.272 mm^2.

Concomitantly, several polished test specimens were subjected to stain resistance testing, according to the procedures of the ISO 10545-14 standard.[16] The staining agents used here were chrome green (an oily solution containing 40 wt.% of Cr_2O_3 – as recommended by the standard) and earth (an aqueous solution containing 50 wt.% of red earth – simulating conditions found in everyday situations).

The intensity of the stains was evaluated from the difference in color ΔE^*, of the surface prior to staining and after the cleaning steps applied on the region where the staining agents had been applied.[17] The values of ΔE^* were determined by diffuse reflectance spectrophotometry (Konica Minolta CM – 2600d), using a standard 10° colorimetric observer and a standard D65 light source (equivalent to daylight). The higher the value of ΔE^* the more intense the stain observed on the surface. Determination of stain intensity by spectrophotometry has proved very efficient in the evaluation of the staining tendency of ceramic tiles, according to recent works.[3,15,18]

It should be noted that the test specimens selected for the SEM analysis were the ones sintered at the temperature at which the highest densification of the material was reached (Section 3.4).

3. Results and discussion

3.1. Progressive surface wear

Table 3 describes the milling parameters used in the preparation of the suspensions with different residues and the resulting values of ρ_S and ρ_R. Note that, as the milling time increases, the amount of particle residues retained in the sieve with 45 μm openings decrease, indicating the increasing degree of comminution achieved. The density of the suspensions, ρ_S, did not show major variations, since the volume of water and the mass of solids used in their preparation were constant.

As mentioned in Section 2.2, the feldspar suspensions were mixed with suspension F1. The exact volume of each mixed suspension was calculated based on Eq. (1), using the values of ρ_S and ρ_R listed in Table 3. To facilitate the identification of the suspensions obtained after completing the mixtures, the following acronyms were established:

Table 3
Milling parameters and properties of the suspensions.

Suspensions	Milling time (min)	Residue in a sieve with 45 μm openings (in wt.%)	ρ_S (g/cm^3)	ρ_R (g/cm^3)
STD	14.0	0.5	1.66	2.835 ± 0.001
	21.0	2.1	1.67	2.835 ± 0.001
Feldspar	18.5	4.3	1.66	2.898 ± 0.002
	12.5	8.9	1.66	2.898 ± 0.002
F1	12.0	0.5	1.65	2.853 ± 0.001

- Fdsp 2.1%: feldspar suspension with 2.1% of residue added to suspension F1;
- Fdsp 4.3%: feldspar suspension with 4.3% of residue added to suspension F1; and
- Fdsp 8.9%: feldspar suspension with 8.9% of residue added to suspension F1.

In addition, the suspension of the STD paste with 0.5% of residue was denoted as: Mass 0.5%.

3.2. Effect of milling on PSD

As the milling time increases, the average size of the particles that make up a ceramic paste should be reduced, leaving behind smaller amounts of residue in the sieve with 45 μm openings. Fig. 1a depicts the PSD graph obtained for the mixture of the suspensions with different amounts of feldspar residues (Fdsp 2.1%, Fdsp 4.3% and Fdsp 8.9%) and for the suspension of the standard paste (Mass 0.5%). Note that increasing the degree of milling (lower residue in the sieve with 45 μm openings) causes the average size of the feldspar particles to decrease.

Table 4 describes the main evaluation parameters of the PSD curves, among which D_{50} stands out for being a statistical parameter that represents the mean particle diameter when the percent cumulative mass is equal to 50%. The highest values of D_{50} are associated with a lower efficiency reached in the milling process.

3.3. Effect of PSD on the green microstructure

Fig. 1b presents the graphs obtained by mercury porosimetry, while Table 5 lists the values of apparent density (ρ_C) of the green test specimens and the volume of Hg intruded in each evaluated condition.

A comparison of the Hg porosimetry curves (Fig. 1b) and the PSD curves (Fig. 1a) indicates that the use of different PSD for a given ceramic body significantly alters the pore volume of the green test specimens produced by compaction. In this context, the data in Table 5 confirm that the increase in the value of D_{50}

Table 4
Evaluation parameters of the PSD curves according to Fig. 1.

Suspensions	D_{50} (μm)	<10 μm (%)	<1 μm (%)
Mass 0.5%	3.9	74.5	8.5
Fdsp 2.1%	3.0	82.5	9.0
Fdsp 4.3%	4.1	72.5	8.1
Fdsp 8.9%	4.8	67.7	7.8

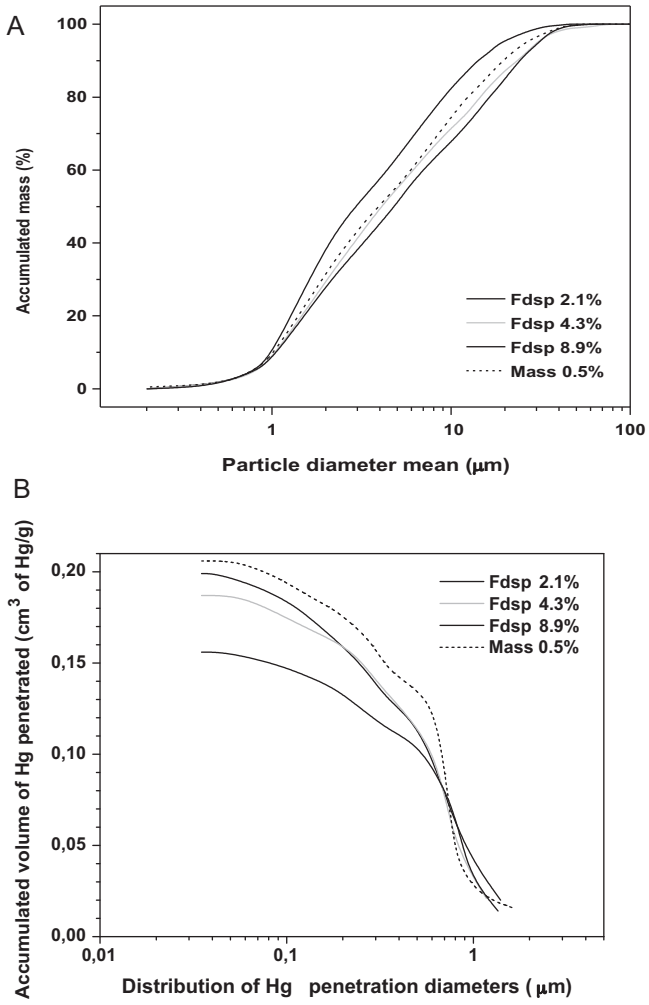

Fig. 1. (a) PSD of feldspar milled in different residues in sieve with 45 μm openings. Comparison against the standard Mass 0.5%; (b) distribution of the mercury intrusion diameters in the green test specimens.

Table 5
Values of apparent density (ρ_C) and accumulated volume of intruded Hg.

Green test specimens	ρ_C (g/cm^3)	Accumulated volume of intruded Hg (cm^3 of Hg/g)
Mass 0.5%	1.67 ± 0.01	0.206
Fdsp 2.1%	1.68 ± 0.01	0.199
Fdsp 4.3%	1.69 ± 0.01	0.197
Fdsp 8.9%	1.70 ± 0.01	0.156

(Table 4) is accompanied by a discrete increase in ρ_C and a decrease in the volume of Hg intruded in the test specimens. In other words, the use of suspensions containing coarser feldspar particles contributes to increase the degree of densification of the green compact, since the volume of pores generated is lower and ρ_C is higher.

These results are consistent with reports in the literature and confirm that the use of larger particles increases the apparent density of the green compact. This is due to the more efficient packing of this type of particle inside the granules during the granulation stage (Section 2.3), favoring the obtainment of granules with a smaller volume of intragranular pores.

As for the distribution of diameters of Hg intrusion, it was found that the Fdsp 2.1%, Fdsp 4.3%, Fdsp 8.9% and Mass 0.5% test specimens presented similar profiles, although the volume of intruded Hg differed (Fig. 1b). This indicates that the distinct feldspar milling conditions used in this work led to greater changes in the volume of pores in the green compacts than in the distribution their diameters.

3.4. Sintering of the test specimens

The sintering temperatures of the compositions were defined using the densification curves (four different temperatures) to determine the firing temperature that maximizes the densities of the fired bodies.

Densification curves were built (Fig. 2) based on the values of WA and LS obtained, and the following T_{max} were selected: Mass 0.5% = 1200 °C; Fdsp 2.1% = 1230 °C; Fdsp 4.3% = 1230 °C; and Fdsp 8.9% = 1250 °C.

With regard to the standard paste (Mass 0.5%), the use of coarser feldspar particles (Fig. 2) caused a gradual increase in the

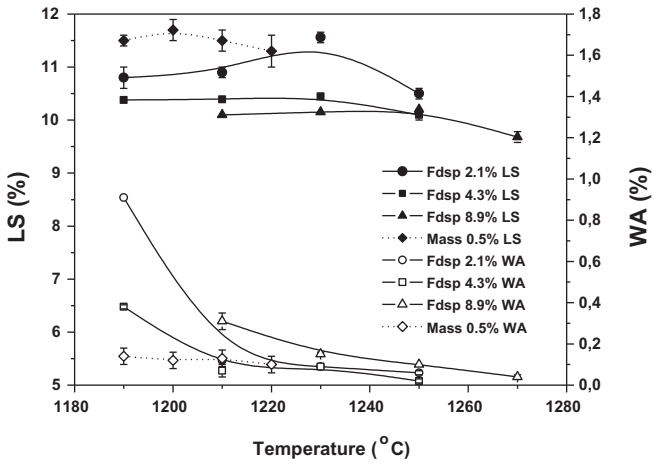

Fig. 2. Variation of linear shrinkage (LS) and water absorption (WA) with sintering temperature of the test specimens.

T_{max}, making it less reactive. Because the densification process during sintering of the porcelain body involves the formation of liquid phase, the larger the size of feldspar particles the smaller the free specific surface that participates in the sintering process, which increases the maximum densification temperature of the material.

3.5. Physical characterization of the sintered test specimens

The test specimens subjected to physical characterization were the ones sintered at T_{max}, which was determined based on the densification curves (Fig. 2).

Table 6 presents the values of WA, LS, ε_A, ε_F, ε and ϕ of the analyzed test specimens. Comparing the porosity of the standard Mass 0.5% with that presented by Fdsp 2.1%, it is clear that the

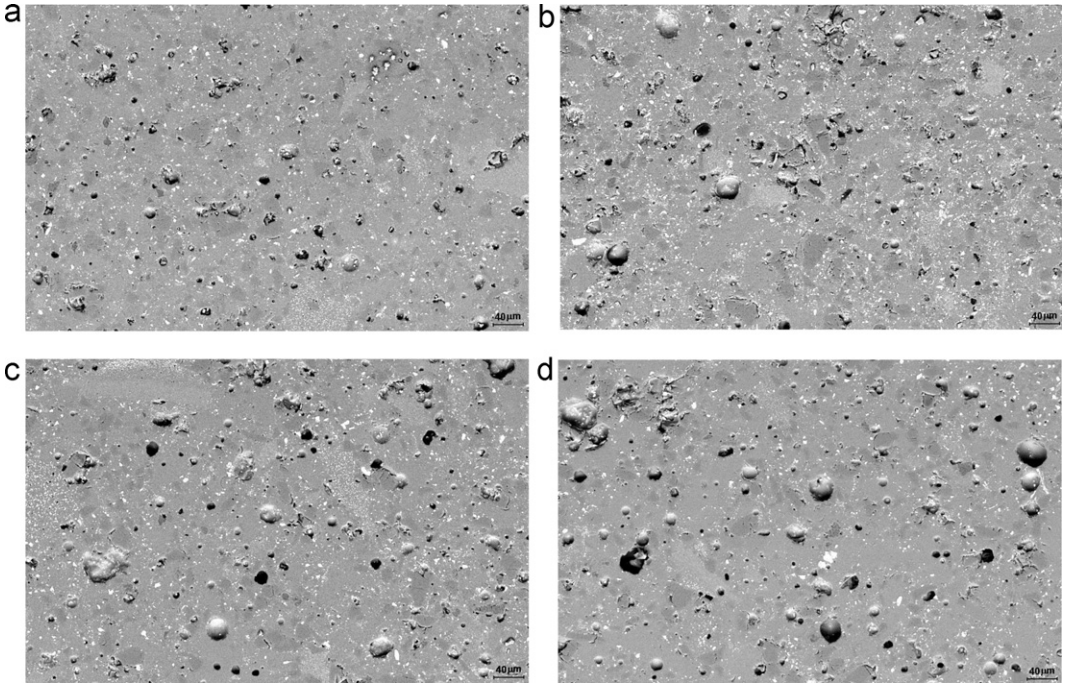

Fig. 3. SEM micrographs of the surfaces of the polished test specimens: (a) Mass 0.5%, (b) Fdsp 2.1%, (c) Fdsp 4.3%, and (d) Fdsp 8.9%.

Table 6
Physical characterization of the sintered test specimens.

Test specimens	WA (%)	LS (%)	ε_A (%)	ε_F (%)	ε[a] (%)	ϕ
Mass 0.5%	0.12 ± 0.04	11.7 ± 0.2	0.21 ± 0.09	9.42 ± 0.12	9.63 ± 0.10	0.92
Fdsp 2.1%	0.09 ± 0.00	11.6 ± 0.1	0.22 ± 0.05	8.44 ± 0.07	8.66 ± 0.06	0.93
Fdsp 4.3%	0.09 ± 0.00	10.5 ± 0.0	0.21 ± 0.06	10.60 ± 0.07	10.81 ± 0.07	0.91
Fdsp 8.9%	0.10 ± 0.00	10.2 ± 0.0	0.26 ± 0.10	12.91 ± 0.10	13.17 ± 0.10	0.89

[a] The value of ρ_R obtained for the calculation of ε was 2.690 g/cm^3.

Fdsp 2.1% test specimens exhibit lower values of ε_F and ε, and slightly higher ϕ, despite their higher content of feldspar milling residue. Among the compositions with different feldspar milling residues, the results show that the use of coarser particles causes the LS to decrease and the ε_F to increase. This indicates that the decrease in the degree of densification ϕ of the test specimens is a result of the presence of coarse pores in the green bodies of this paste. These kinds of pores are more difficult to eliminate during the vitrification process.[6,8,9]

A comparison of the characteristics of the green compacts (Table 5) with the results obtained for the sintered test specimens (Table 6) reveals that the pastes that initially presented the highest pore volumes were the ones that reached the highest degree of densification during sintering. This is due to the fact that, although the use of fine particles is the main cause for lower packing of the green compact, during sintering this type of particle enhances the reactivity of the material and of the content of the liquid phase, contributing to the process of densification.

3.6. Analysis of SEM images and staining

Fig. 3 presents the SEM micrographs of the surfaces of the polished test specimens.

The results of the image analysis were organized on graphs of pore diameter distribution (Fig. 4a) and aspect ratio (Fig. 4b) as a function of cumulative percent of pores. For the correct interpretation of Fig. 4a and b should be considered that the more displaced upward (vertical axis) the analyzed point is chosen, the greater is the percentage of accumulated pore: (a) with smaller diameters than those displayed on the horizontal axis (Fig. 4a); and (b) with smaller aspect ratios than those displayed on the horizontal axis (Fig. 4b).

Table 7 lists the percent of pores per unit area of the polished surface with the values of ΔE^* after the stain resistance test.

Based on the results of the analysis of the images and staining, the following comments deserve highlighting:

Table 7
Results of image analysis and ΔE^*.

Polished test specimens	Pores per unit area (%)	ΔE^*
Mass 0.5%	4.51 ± 0.40	1.93
Fdsp 2.1%	4.32 ± 0.76	1.34
Fdsp 4.3%	5.51 ± 0.64	5.77
Fdsp 8.9%	6.71 ± 0.93	6.12

- Among the Fdsp pastes, the least effective milling of feldspar contributed to a discrete increase in the average pore diameter observed in the sintered material. This tendency was accompanied by an increase in the space occupied by pores in relation to the area in the images as the milling residue increased. The values of ΔE^* were also found to increase along with the increase in milling residue, i.e., surface cleanability is impaired by the decrease in the degree of milling.
- Upon comparing the results of stain resistance of the Fdsp pastes with the standard Mass 0.5% paste, one finds that the Fdsp 2.1% composition presented a slightly better stain

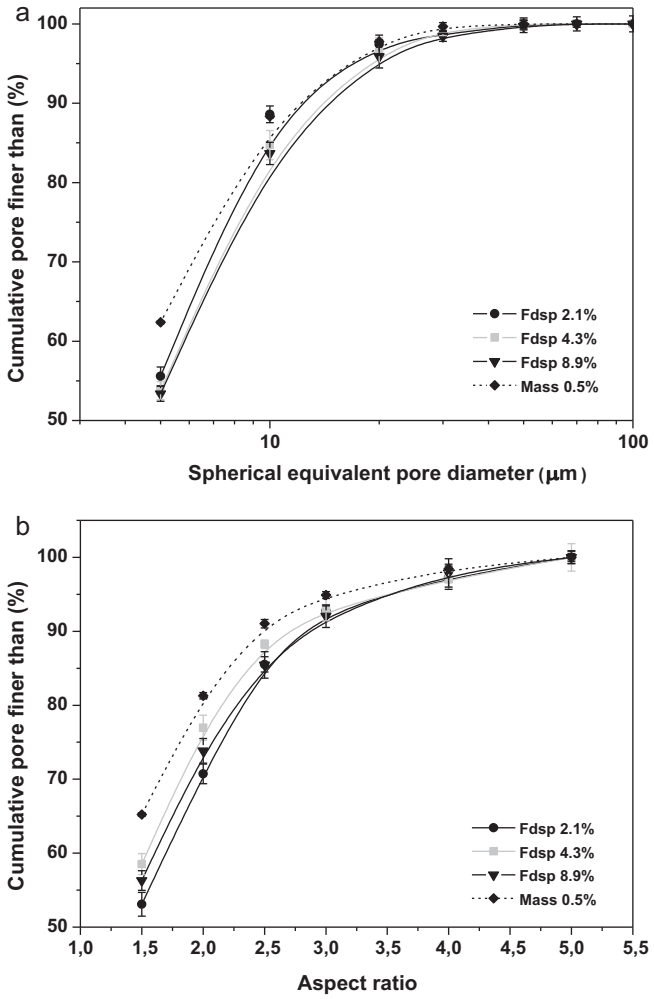

Fig. 4. (a) Pore diameter distribution on the surface of the polished test specimens; and (b) distribution of the values of the aspect ratio of pores on the surface of polished test specimens.

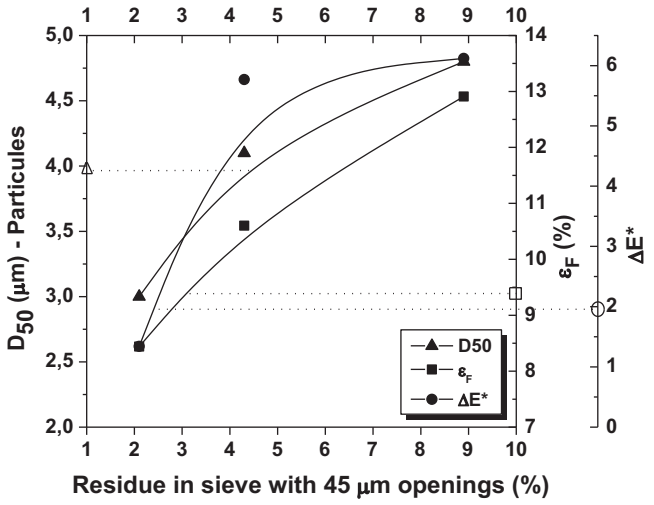

Fig. 5. Variation of D_{50}, ε_F and ΔE^* according to feldspar milling residues. Highlighted points on the axes: values presented by the Mass 0.5% standard.

resistance than the standard, since the ΔE^* values obtained were lower. This indicates that less controlled milling of feldspar, with residues of up to 2.1% in the sieve with 45 μm openings, is feasible. In this case, the values of ΔE^* seem to depend more on the pore area than on their diameter distribution and morphology. This statement is based on the fact that, although the surfaces of Mass 0.5% presented pores with smaller diameters (Fig. 4a) and shapes tending toward the spherical (Fig. 4b), the polished surfaces of the Fdsp 2.1% test specimens showed the best result, i.e., the lowest percent of pores per unit area.

3.7. Relationship between the PSD of feldspar and post-sintering properties

To facilitate the interpretation of the results, a graph was created to evaluate the individual participation of feldspar in the formation of closed pores and staining (Fig. 5).

As can be seen in Fig. 5, the decrease in the degree of milling of feldspar causes an increase in the average size of the particles that will make up the granules of the material. Although the degree of densification of the green compact is higher in these conditions, the increase in D_{50} is accompanied by an increase in the percentage of closed pores due to the lower reactivity of the body during sintering. Polishing the sintered test specimens reveals the closed pores at the surface and acts negatively on the stain resistance of the specimens, increasing the intensity of stains as the number of pores increases (higher percentage). It was found that a minor variation in feldspar milling residue can significantly alter the pore volume and cleanability of the polished surface.

4. Conclusions

The results of this work led to the following conclusions:

- The degree of densification of the green compact may vary according to the PSD of the raw materials that make up the feldspar body. As the milling time decreases, the average particle size increases, favoring the formation of denser granules during the granulation stage. In such conditions, the green compact reaches higher values of apparent density due to the better packing of particles. However, the use of particles with larger diameters causes the volume and diameter of closed pores to increase due to the lower reactivity attained during sintering, thus worsening the cleanability of the polished surface.
- Slight variations in the average particle size of feldspar can lead to significant changes in the porous microstructure of the final product, thereby modifying its stain resistance. Under the conditions adopted in this work, it is possible to incorporate feldspar in porcelain paste with a milling residue of up to 2.5% retained in an sieve with 45 μm openings (according to the tendency illustrated in Fig. 5), without impairing the product's stain resistance, and even achieve a discrete reduction in the intensity of staining when compared with the STD paste.

References

1. Dondi M, Raimondo M, Zanelli C. Stain resistance of ceramic tiles. *Ceram World Rev* 2008;**77**:82–9.
2. Cavalcante PMT, Dondi M, Ercolani G, Guarini G, Melandri C, Raimondo M, Amendra E. The influence of microstructure on the performance of white porcelain stoneware. *Ceram Int* 2004;**30**:953–63.
3. Dondi M, Ercolani G, Guarini G, Melandri C, Raimondo M, Rocha e Almendra E, Cavalcante PMT. The role of surface microstructure on the resistance to stains of porcelain stoneware tiles. *J Eur Ceram Soc* 2005;**25**: 357–65.
4. Alves HJ, Minussi FB, Melchiades FG, Boschi AO. Characteristics of pores responsible for staining of polished porcelain tile. *Ind Ceram* 2011;**31**:21–6.
5. Beltrán V, Ferrer C, Bagán V, Sánchez E, Garcia J, Mestre S. Influence of pressing powder characteristics and firing temperature on the porous microstructure and stain resistance of porcelain tile. In: *Proceedings of the IV world congress on ceramic tile quality*. 1996. pp. 133–48.
6. Amorós JL, Cantavella V, Jarque JC, Felíu C. Fracture properties of spray-dried powder compacts: effect of granule size. *J Eur Ceram Soc* 2008;**28**:2823–34.
7. Alves HJ, Melchiades FG, Boschi AO. Effect of spray-dried powder granulometry on the porous microstructure of polished porcelain tile. *J Eur Ceram Soc* 2010;**30**:1259–65.
8. Amorós JL, Orts MJ, García-Ten J, Gozalbo A, Sánchez E. Effect of the green porous texture on porcelain tile properties. *J Eur Ceram Soc* 2007;**27**:2295–301.
9. Martín-Márques J, Rincón J, Ma Romero M. Effect of firing temperature on sintering of porcelain stoneware tiles. *Ceram Int* 2008;**34**(8):1867–73.
10. Suvaci E, Tamsu N. The role of viscosity on microstructure development and stain resistance in porcelain stoneware tiles. *J Eur Ceram Soc* 2010;**30**:3071–7.
11. Bernardin AM, Medeiros DS, Riella HG. Pyroplasticity in porcelain tiles. *Mater Sci Eng A* 2006;**427**:316–9.
12. International Standard ISO 10545-3. *Ceramic tile – part 3: determination of water absorption, apparent porosity, apparent relative density and bulk density*; 1997.
13. Hutchings IM, Xu Y, Sánchez E, Ibáñez MJ, Quereda MF. Porcelain tile microstructure: implications for polishability. *J Eur Ceram Soc* 2006;**26**:1035–42.

14. Jazayeri SH, Salem A, Timellini G, Rastelli E. A kinetic study on the development of porosity in porcelain stoneware tile sintering. *Boletin de la Sociedad Española de Cerámica y Vidrio* 2007;**46**(1):1–6.
15. Alves HJ, Freitas MR, Melchiades FG, Boschi AO. Dependence of surface porosity on the polishing depth of porcelain stoneware tiles. *J Eur Ceram Soc* 2011;**31**:665–71.
16. International Standard ISO 10545-14. *Ceramic tiles – part 14: determination of resistance to stains*; 1997.
17. Rastelli E, Tucci A, Esposito L, Selli S. Stain resistance of porcelain stoneware tile: mechanisms of penetration of staining agents and quantitative evaluation. *Ceram Acta* 2002;**14**(1):30–7.
18. Sánchez E, Ibáñez MJ, García-Ten J, Quereda MF, Hutchings IM, Xu YM. Porcelain tile microstructure: implications for polished tile properties. *J Eur Ceram Soc* 2006;**26**:2533–40.